An Atomistic Perspective on Biomolecular Adsorption on Functionalized Carbon Nanomaterials at Ambient Conditions

Supporting Information

Marzieh Saeedimasine, Erik G. Brandt, and Alexander P. Lyubartsev*

Department of Materials and Environmental Chemistry, Stockholm University, Stockholm, Sweden

E-mail: alexander.lyubartsev@mmk.su.se

Modification of GAFF parameters for the carbon nanomaterials

We have modified the original GAFF parameters for carbon nanomaterials according to the following considerations. First, we use the established C−C bond length, $a = 0.142\,\mathrm{nm}$ (used also in Amber03 force field), for the bonds between carbon atoms in the CNTs and graphene. The equilibrium value in GAFF derived from benzene is 2 % smaller. The force constants were taken directly from GAFF for CA type of atoms. Second, we used bond lengths between the CNT and the functionalized groups from the *ab initio* calculations of Milowska and Majewski[1] and Veloso et.al.[2] The force constants were taken extracted from the bonds between the corresponding atom types in the AMBER03 force field.[3] Third, the equilibrium angles of the COO(H)-groups were calibrated slightly to match the *ab initio* calculations of Lara et al.,[4] which shows that the angles in the functionalizing group contracts angles when attached to the CNT surface compared to in vacuum.

These tweaks improve the agreement with available *ab initio* calculations of bonding between CNTs and functionalizing groups, in comparison to the parameterization of the molecular fragments. The bonded force field parameters for the functionalized CNTs are given in Tables S1 ans S2.

Table S1: Modified GAFF parameters for bonded atoms in the functionalized CNT. Bond equilibrium lengths, b_0, and bond force constants, k_b, were extracted from GAFF based on molecular fragments. The equlibrium bond lengths between the CNT and the functionalizing group were obtained from previous *ab initio* calculations.[1,2] b_0 is in nm and k_b is in $\mathrm{kJ\,mol^{-1}\,nm^{-2}}$.

i	j	b_0	k_b	Description	Source
C_A	C_A	0.1420	392459.2	aromatic C−C in CNT	b_0 from Ref.,[1] k_b from AMBER03[3]
C_A	C_B	0.1420	392459.2	aromatic C−C in CNT	b_0 from Ref.,[1] k_b from AMBER03[3]
C_A	C_C	0.1420	392459.2	aromatic C−C in CNT	b_0 from Ref.,[1] k_b from AMBER03[3]
C_A	C_D	0.1420	392459.2	aromatic C−C in CNT	b_0 from Ref.,[1] k_b from AMBER03[3]
C_B	O_A	0.1450	267776.0	CNT to OH	b_0 from Ref.,[1] k_b from AMBER03[3]
C_C	C_E	0.1560	259408.0	CNT to COO(H)	b_0 from Ref.,[1] k_b from AMBER03[3]
C_D	N_A	0.1490	282001.6	CNT to NH2	b_0 from Ref.,[2] k_b from AMBER03[3]
C_D	N_B	0.1490	282001.6	CNT to NH3+	b_0 from Ref.,[2] k_b from AMBER03[3]
C_E	O_A	0.1364	376560.0	C−O in COO(H)	GAFF
C_E	O_B	0.1229	476976.0	C=O/C−O^- in COO(H)	GAFF
O_A	H_A	0.0960	462750.4	O−H in OH	GAFF
N_A	H_B	0.1010	363171.2	N−H in NH_2	GAFF
N_B	H_B	0.1010	363171.2	N−H in NH_3^+	GAFF

Table S2: Parameters for atoms connected with two bonds (angular potentials) in the functionalized carbon nanotube force field. Angle equilibrium lengths, θ_0, and angle force constants, k_θ, were extracted from GAFF based on molecular fragments. The equilibrium angles in the functionalized COO(H)-groups were obtained from previous *ab initio* calculations.[4] θ_0 is in degrees and k_θ is in $\mathrm{kJ\,mol^{-1}\,rad^{-2}}$.

i	j	k	θ_0	k_θ	Description	Source
C_A	C_A	C_A	120.0	527.184	∠C−C−C at linker in CNT (sp2)	GAFF
C_A	C_A	C_B	120.0	527.184	∠C−C−C at linker in CNT (sp2)	GAFF
C_A	C_A	C_C	120.0	527.184	∠C−C−C at linker in CNT (sp2)	GAFF
C_B	C_A	C_B	120.0	527.184	∠C−C−C at linker in CNT (sp2)	GAFF
C_B	C_A	C_C	120.0	527.184	∠C−C−C at linker in CNT (sp2)	GAFF
C_C	C_A	C_C	120.0	527.184	∠C−C−C at linker in CNT (sp2)	GAFF
C_A	C_B	C_A	109.5	334.720	∠C−C−C at adsorption site in CNT (sp3)	GAFF
C_A	C_B	O_A	109.5	418.400	∠C−C−O from CNT to OH (sp3)	GAFF
C_A	C_C	C_A	109.5	334.720	∠C−C−C from CNT to COO(H) (sp3)	GAFF
C_A	C_C	C_E	109.5	334.720	∠C−C−C from CNT to COO(H) (sp3)	GAFF
C_A	C_D	N_A	109.5	669.440	∠C−C−N from CNT to NH_2 (sp3)	GAFF
C_A	C_D	N_B	109.5	669.440	∠C−C−N from CNT to NH_3^+ (sp3)	GAFF
C_C	C_E	O_A	110.0	669.440	∠C−C−O from CNT via C to OH in COO(H)	GAFF
C_C	C_E	O_B	120.0	669.440	∠C−C−O from CNT via C to O/O- in COO^-	GAFF
O_A	C_E	O_B	116.5	669.440	∠O−C−O in COOH	θ_0 from Ref.,[4] k_θ from GAFF
O_B	C_E	O_B	122.5	669.440	∠O−C−O in COO^-	θ_0 from Ref.,[4] k_θ from GAFF
C_B	O_A	H_A	108.5	460.240	∠C−O−H from CNT via O to H in OH	GAFF
C_E	O_A	H_A	120.0	418.400	∠C−O−H in COOH (sp2)	θ_0 from Ref.,[4] k_θ from GAFF
C_D	N_A	H_B	110.0	394.400	∠C−N−H from CNT via N to H in NH_2	GAFF
H_B	N_A	H_B	107.0	345.600	∠H−N−H in NH_2	GAFF
C_D	N_B	H_B	110.0	386.520	∠C−N−H from CNT via N to H in NH_3^+	GAFF
H_B	N_B	H_B	108.0	339.070	∠H−N−H in NH_3^+	GAFF

List of biomolecules for adsorption free energy calculations

1. Aminoacids side chain analogues (except GLY, PRO)

Alanine (ALA): 

Arginine (ARG): 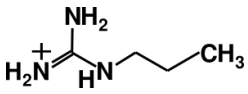

Asparagine (ASN): 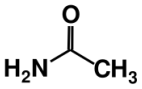

Asparic acid (ASP): 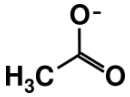

Cysteine (CYS): 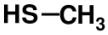

Glutamine (GLN): 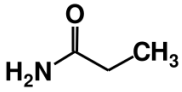

Glutamic acid (GLU): 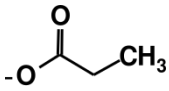

Histidine (HID): 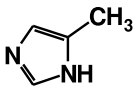

(HIE): 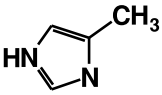

Isoleucine (ILE): 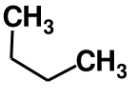

Leucine (LEU): 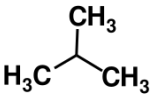

Lysine (LYS): 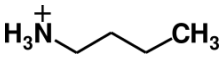

Methionine (MET): 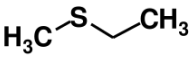

Phenilalanine (PHE): 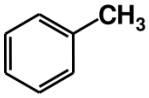

Serine (SER): 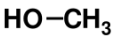

Threonine (THR): 

Tryptophan (TRP): 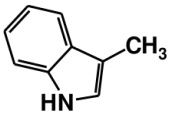

Tyrosine (TYR): 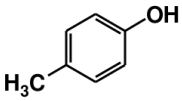

Valine (VAL): 

2. GLY and PRO aminoacids (with backbone)

Glycine (GLY) 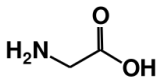

Proline (PRO) 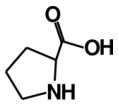

3. Alternative forms (4<pKa<10)

Histidine ion (HIP)
Ph < 6 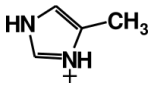

Glutamic acid neutral
(GAN) ph < 4.3 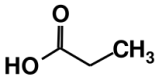

Cysteine- (CYM):
ph > 8.4 

4. Lipid fragments

Choline (CHL) 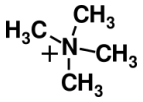

Etanolamine (ETA) 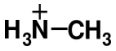

Phosphate (PHO) 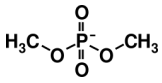

Esters (EST) 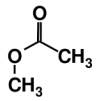

5. Glucose

D-glucose (DGL) 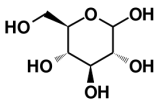

Figure S1: List of biomolecules for adsorption free energy calculations on carbon nanomaterials

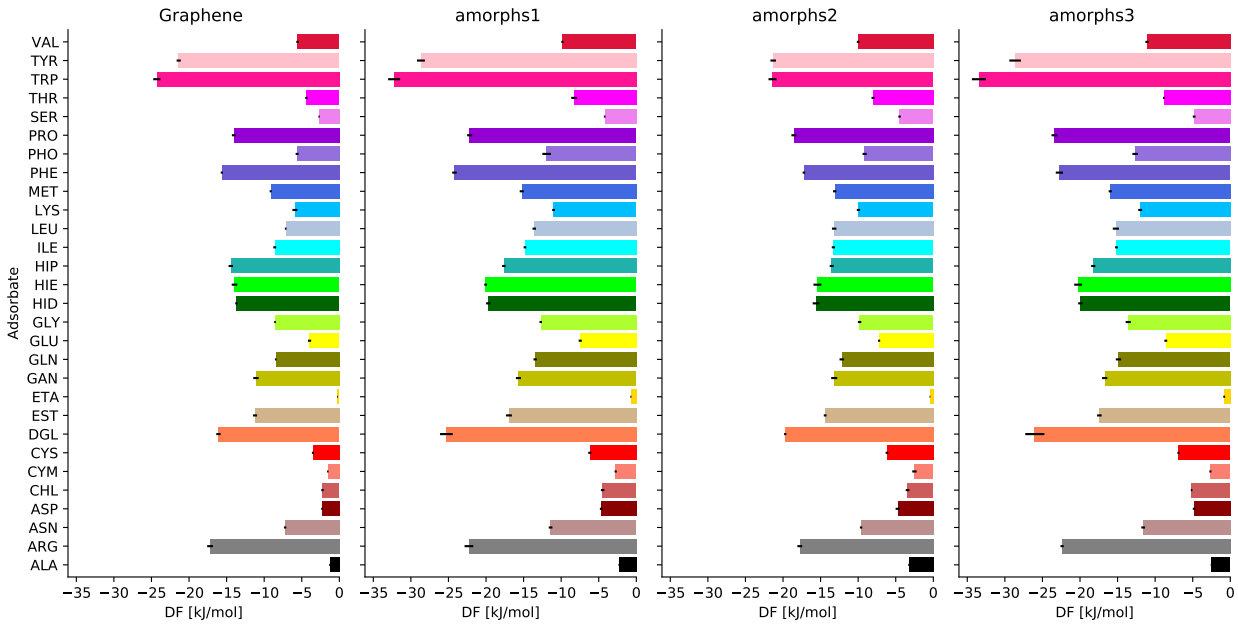

Figure S2: Binding free energies of biomolecules on graphene and three different ta-C slabs.

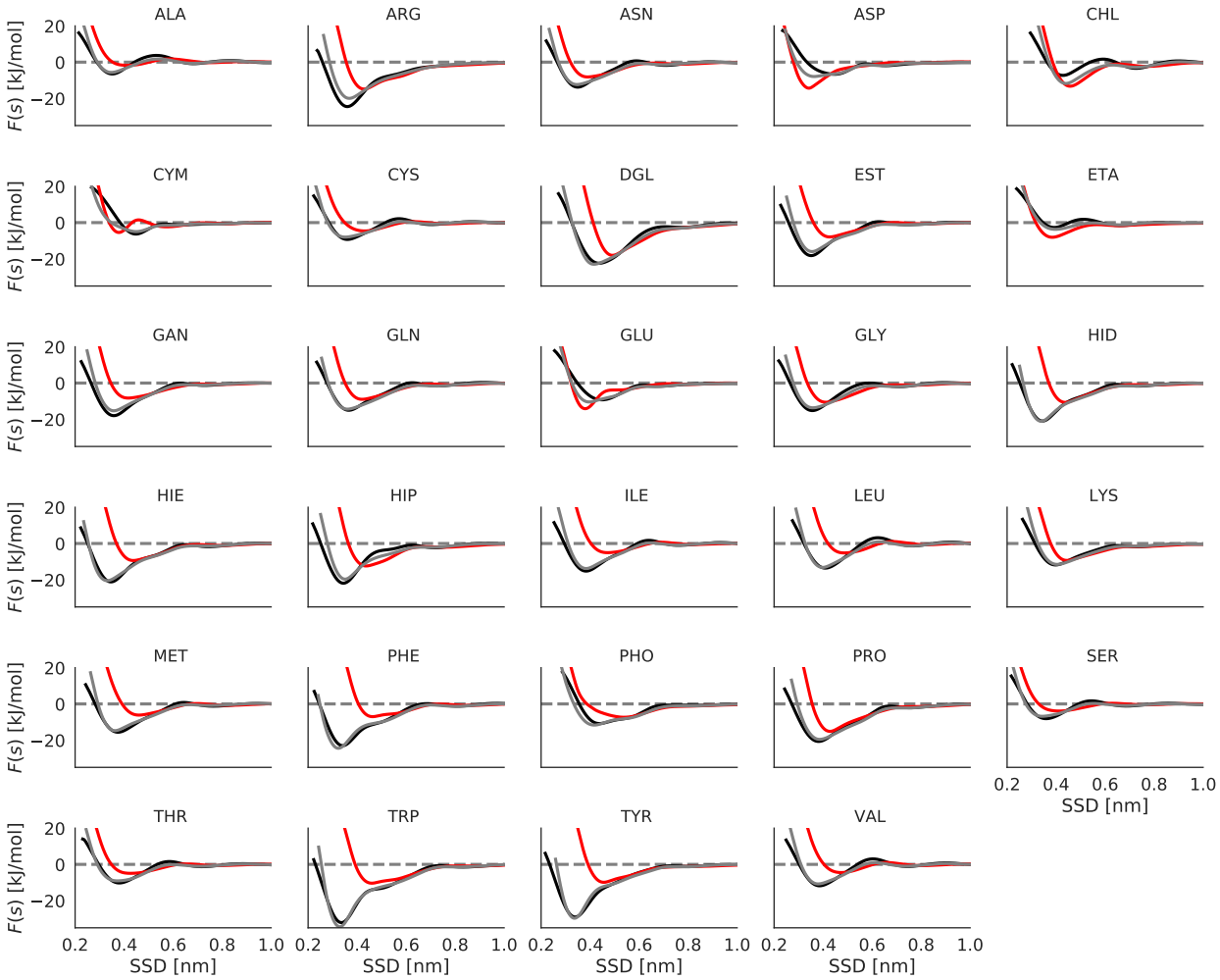

Figure S3: Adsorption profile of different biomolecules on graphene **(black)**, grapheneoxide **(red)**, and reduced grapheneoxide**(gray)**.

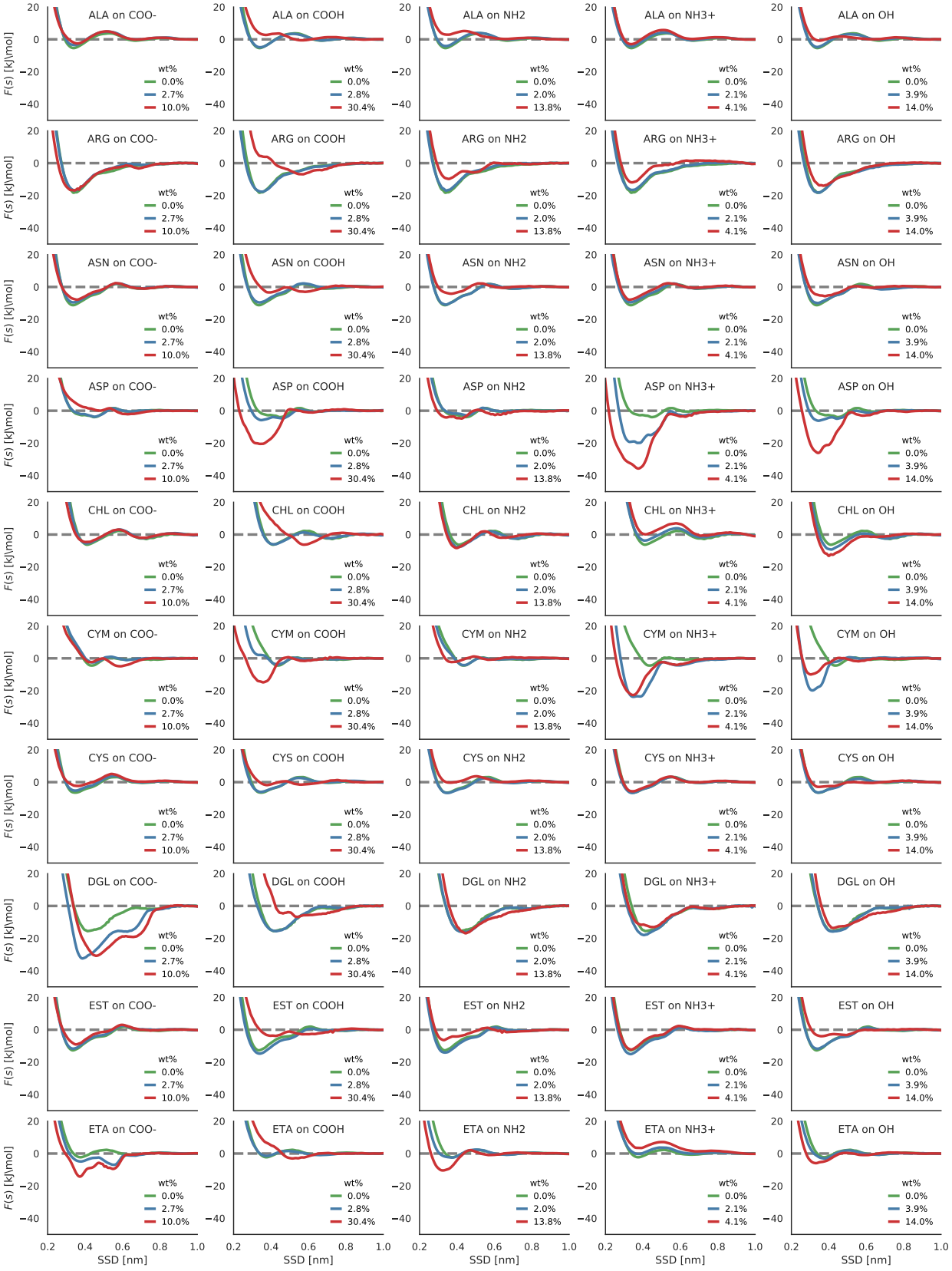
ALA on COO-
ALA on COOH
ALA on NH2
ALA on NH3+
ALA on OH
ARG on COO-
ARG on COOH
ARG on NH2
ARG on NH3+
ARG on OH
ASN on COO-
ASN on COOH
ASN on NH2
ASN on NH3+
ASN on OH
ASP on COO-
ASP on COOH
ASP on NH2
ASP on NH3+
ASP on OH
CHL on COO-
CHL on COOH
CHL on NH2
CHL on NH3+
CHL on OH
CYM on COO-
CYM on COOH
CYM on NH2
CYM on NH3+
CYM on OH
CYS on COO-
CYS on COOH
CYS on NH2
CYS on NH3+
CYS on OH
DGL on COO-
DGL on COOH
DGL on NH2
DGL on NH3+
DGL on OH
EST on COO-
EST on COOH
EST on NH2
EST on NH3+
EST on OH
ETA on COO-
ETA on COOH
ETA on NH2
ETA on NH3+
ETA on OH
F(s) [kJ\mol]
SSD [nm]
wt%
0.0%
2.7%
10.0%
2.8%
30.4%
2.0%
13.8%
2.1%
4.1%
3.9%
14.0%

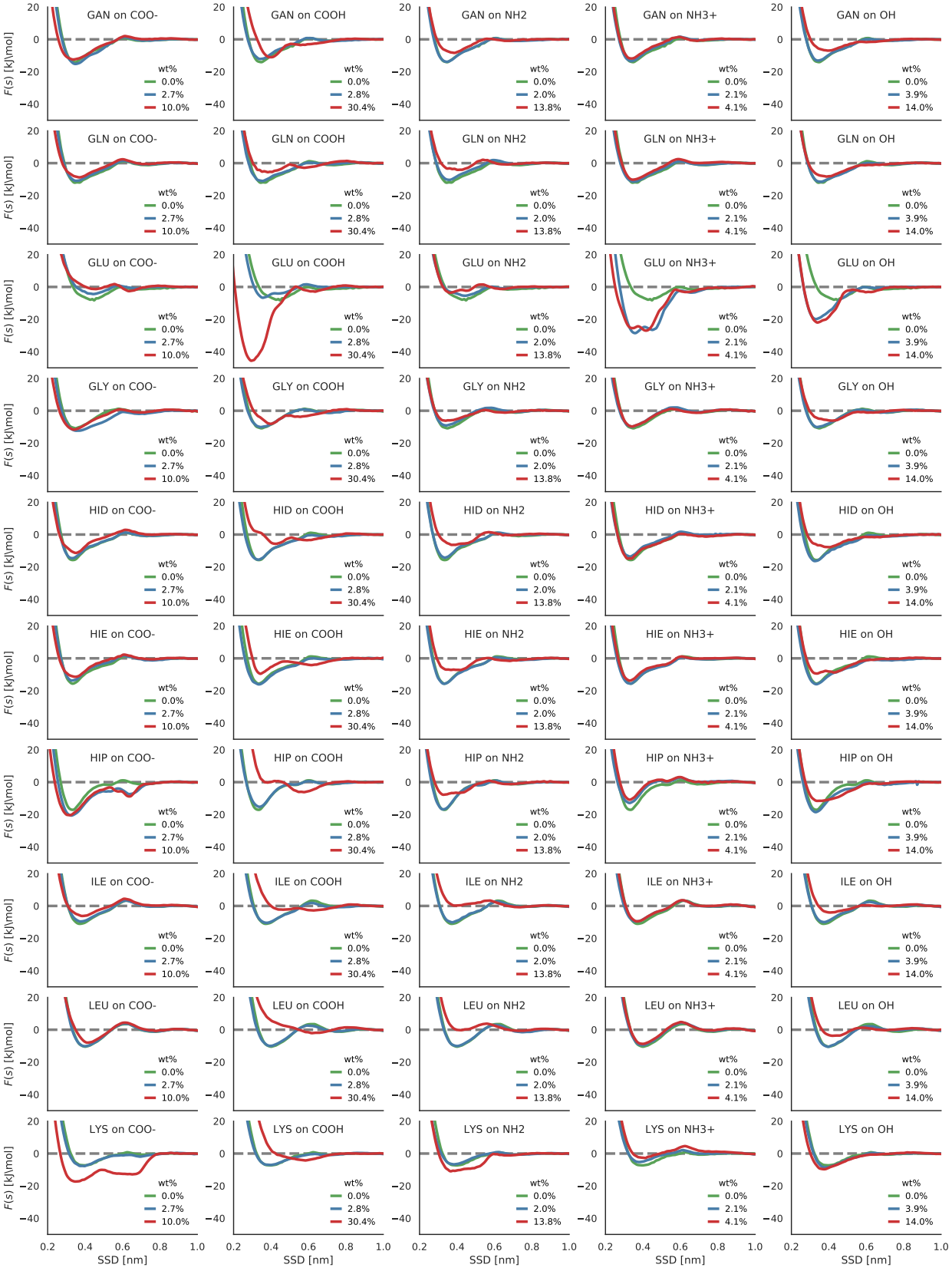
GAN on COO-
wt%
0.0%
2.7%
10.0%
GAN on COOH
wt%
0.0%
2.8%
30.4%
GAN on NH2
wt%
0.0%
2.0%
13.8%
GAN on NH3+
wt%
0.0%
2.1%
4.1%
GAN on OH
wt%
0.0%
3.9%
14.0%
GLN on COO-
GLN on COOH
GLN on NH2
GLN on NH3+
GLN on OH
GLU on COO-
GLU on COOH
GLU on NH2
GLU on NH3+
GLU on OH
GLY on COO-
GLY on COOH
GLY on NH2
GLY on NH3+
GLY on OH
HID on COO-
HID on COOH
HID on NH2
HID on NH3+
HID on OH
HIE on COO-
HIE on COOH
HIE on NH2
HIE on NH3+
HIE on OH
HIP on COO-
HIP on COOH
HIP on NH2
HIP on NH3+
HIP on OH
ILE on COO-
ILE on COOH
ILE on NH2
ILE on NH3+
ILE on OH
LEU on COO-
LEU on COOH
LEU on NH2
LEU on NH3+
LEU on OH
LYS on COO-
LYS on COOH
LYS on NH2
LYS on NH3+
LYS on OH
F(s) [kJ\mol]
SSD [nm]

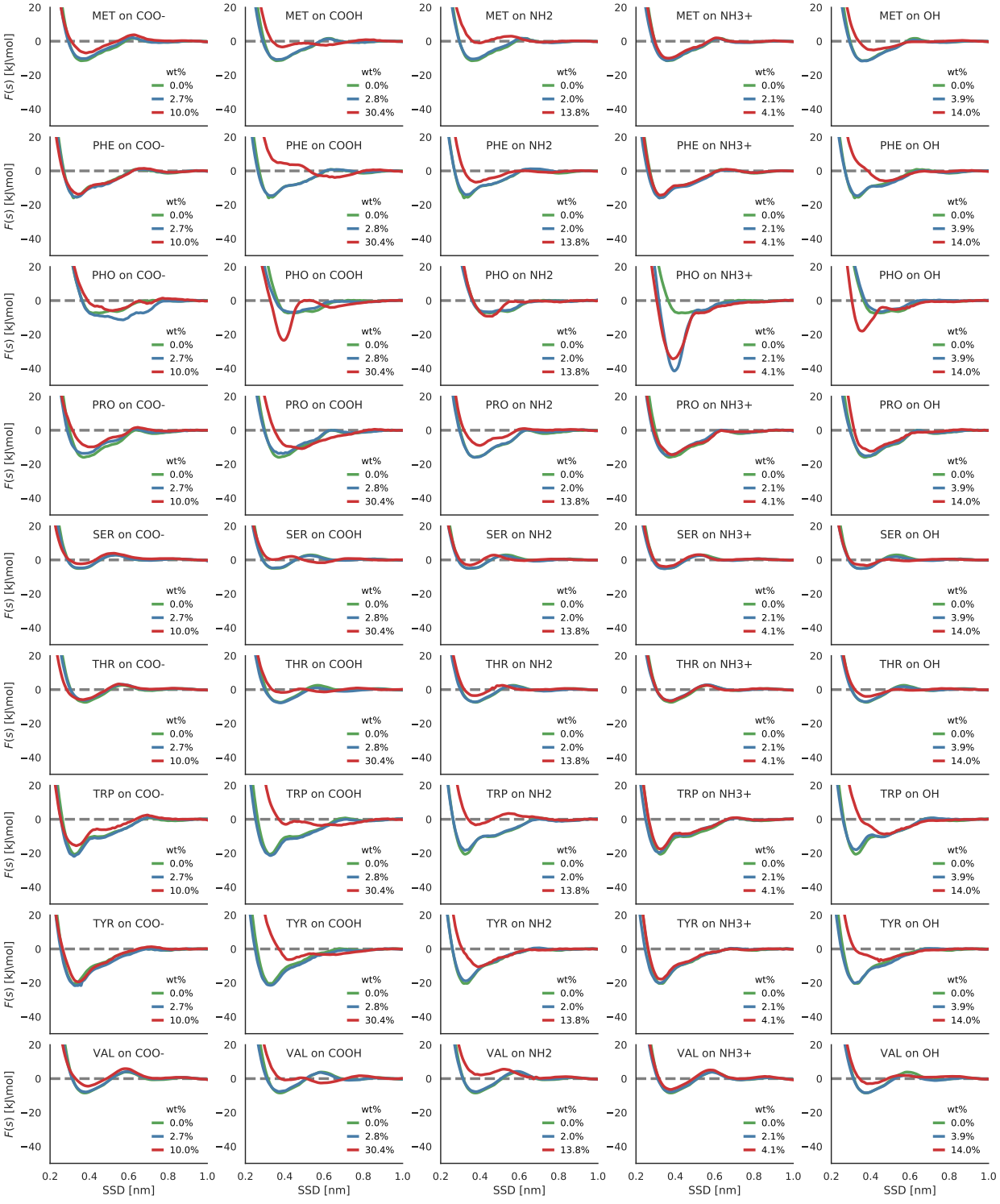

Figure S4: Adsorption profile of different biomolecules on functionalized carbon nanotubes with different groups and different concentrations.

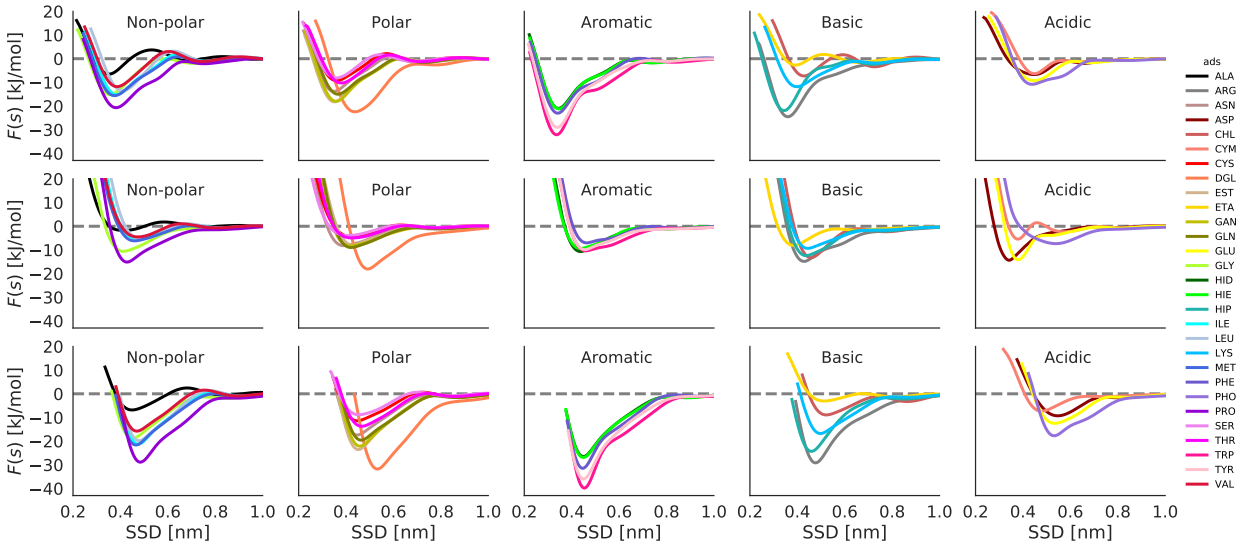

Figure S5: Adsorption profile of all 29 biomolecules grouped into the categories (polar, aromatic, etc) on graphene **(up)**, graphene oxide **(middle)**, and amorphous carbon**(down)**.

Evaluation of convergence of the simulations and uncertainty of the computed data

We assessed the convergence of the adsorption profiles obtained in AWT-MetaD simulations with statistical forecasting. The analysis is based on the time series,

$$\Delta F_{\text{ads}}(t) = -k_B T \ln \left(\frac{1}{\delta} \int_0^{\delta} \mathrm{d}s \, e^{-PMF(s,t)/k_B T} \right) , \tag{1}$$

where $PMF(s,t)$ is the adsorption profile obtained by force integration or cumulatively summing the bias up to time t (so that the "true" adsorption profile is represented by the $t \to \infty$ limit). We ignore systematical errors from flawed modeling and assume that insufficient sampling is the only error source. Then, $\Delta F_{\text{ads}}(t)$ is a correlated time series which converges to a constant value (the binding free energy) in the time limit $t \to \infty$. $\Delta F_{\text{ads}}(t)$ was modeled with an additive regression model using the open source fb-prophet library.[5] The main component of the time series was modeled with a logistic growth curve, instead of a

linear trend, since the time series is known to converge to the binding free energy at long times. The binding free energies of most adsorbates converged after 200 ns simulation time, but some strong binders required substantially longer times (~ 600 ns). All our production metadynamics simulations were run for 300 ns if not said otherwise.

In MetaDF suimulations with constant Gaussian height, the first 50 ns of simulations were excluded from average force computations. The statistical error was calculated from the variance of results obtained within each of 100 ns fragments of the trajectory. Note, that in the force integration method one does not need to wait that the bias potential converged to exactly compensate the free energy profile; it is enough that it provided sampling over the whole range of the collective variable, which was the cases of all simulations carried out in this work.

We have investigated 1D free energy profile of biomolecules on carbon nanomaterial surfaces using AWT-MetaD and MetaDF simulations. These simulations do not impose any restrictions on sidechain orientations, that is why these effects are fully accounted for provided that simulation time is long enough to adequately sample the orientational degrees of freedom. We have prolonged several simulations up to 1000 ns allowing biomolecules to adopt different orientations and conformations with respect to the surface and hydrogen bound to water and functional groups at the surfaces. To validate the PMF convergence, as well as to compare AWT-MetaD and MetaDF, we have computed time series of adsorption profile for different biomolecules categories on different carbon nanomaterial surfaces. The results are shown in Figure S6. For graphene surface, both MetaDF and AWT-MetaD reach the same PMF after 200 ns of the simulations, though PMF profile with AWT-MetaD is slower to be converged. For grapheneoxide surface the PMFs converge typically within 600 ns if computed with MetaDF, but for some stronger binder such as GLU, AWT-MetaD does not show converged profile even at longer simulation time. Since the PMF is not changing by increasing the simulation for different biomolecules categories, it validates that sampling was adequate to produce reliable results.

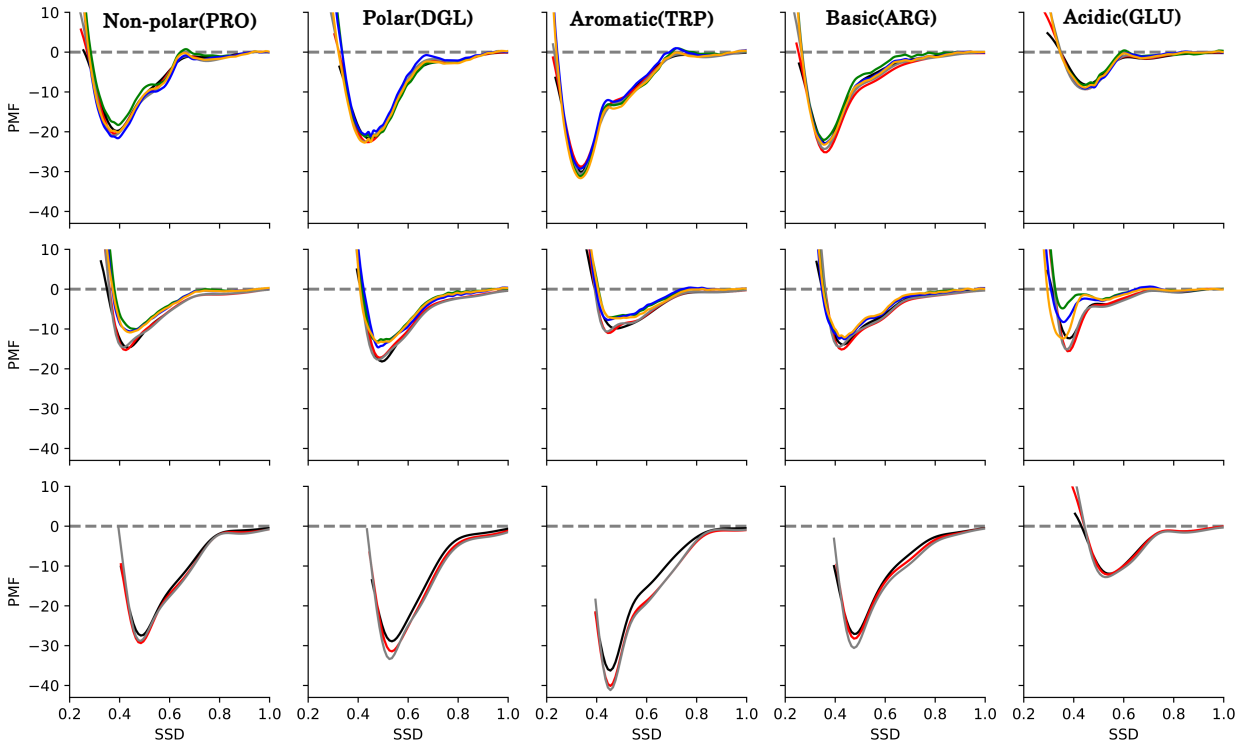

Figure S6: Time evolution of free energy profile for adsorption of representative biomolecule in each group on graphene (Upper row), grapheneoxide (middle row), and amorphous carbon(lower row) surfaces colored as follow. **MetaDF**: black, red, gray at 100 ns, 200 ns, and 300 ns for graphene and amorphous carbon and at 300 ns, 600 ns, and 900 ns for grapheneoxide. **AWT-MetaD**: green, blue, orange at 100 ns, 200 ns, and 300 ns for graphene and at 300 ns, 600 ns, and 900 ns for grapheneoxide.

References

(1) Milowska, K. Z.; Majewski, J. A. Functionalization of Carbon Nanotubes With -CH_n, -NH_n Fragments, -COOH and -OH Groups. *J. Chem. Phys.* **2013**, *138*, 194704.

(2) Veloso, M. V.; Souza Filho, A. G.; Mendes Filho, J.; Fagan, S. B.; Mota, R. Ab Initio Study of Covalently Functionalized Carbon Nanotubes. *Chem. Phys. Lett* **2006**, *430*, 71–74.

(3) Duan, Y.; Wu, C.; Chowdhury, S.; Lee, M. C.; Xiong, G.; Zhang, W.; Yang, R.; Cieplak, P.; Luo, R.; Lee, T.; Caldwell, J.; Wang, J.; Kollman, P. A Point-Charge

Force Field for Molecular Mechanics Simulations of Proteins Based on Condensed-Phase Quantum Mechanical Calculations. *J. Comput. Chem.* **2003**, *24*, 1999–2012.

(4) Lara, I. V.; Zanella, I.; de Souza Filho, A. G.; Binotto Fagan, S. Influence of Concentration and Position of Carboxyl Groups on the Electronic Properties of Single-Walled Carbon Nanotubes. *Phys. Chem. Chem. Phys.* **2014**, *16*, 21602–21608.

(5) Taylor, S. J.; Letham, B. Forecasting At Scale. *Am. Stat.* **2017**, *0*, 0–0.